Acta Geotechnica (2025) 20:1035–1048
https://doi.org/10.1007/s11440-024-02429-2

RESEARCH PAPER

Estimation of compression behavior of granular soils considering initial density effect based on equivalent concept

Yiwen Zeng[1,2] · Xiusong Shi[1,2] · Jidong Zhao[3] · Xia Bian[2] · Jiaying Liu[4]

Received: 8 April 2024 / Accepted: 9 October 2024 / Published online: 6 November 2024

Abstract

Compressibility of granular materials depends on its initial density and is significantly affected by particle breakage, especially at high stress levels. In this study, a simple compression model for granular soils is proposed by incorporating a new equivalent concept. The initial density effect on the curvature of compression line is captured by a novel equivalent void ratio, which features a state variable for describing the evolution of grain crushing and corresponding yielding behavior. An Equivalent Compression Curve (ECC) is further established by directly implementing the equivalent void ratio into a reference compression curve. Validation has been done by comparing the simulated curves with the test data from available literature. It reveals a good linear relationship between the state variable and breakage index. Moreover, the ECC can well normalize the compression behavior of granular soils with a wide range of initial densities and stress levels. The simplified version of ECC includes only three parameters which are consistent with the reference model. The proposed model provides a basis for establishing versatile and rigorous hardening law that can be readily used in conjunction with the general elasto-plasticity theory.

Keywords Granular soils · Compressibility · Equivalent Compression Curve · Equivalent void ratio · Particle breakage

1 Introduction

Granular soils are widely used as construction materials in geotechnical engineering projects, such as slope project, railway subgrades, and roadbed of airports [1–6]. The compressibility of granular materials is crucial for evaluating the workability of those structures, and it has been extensively investigated based on laboratory tests [7–19] and numerical simulations [20–29]. These studies reported that the compressibility of granular material is significantly affected by the current state, i.e., void ratio and stress levels [7, 30, 31]. Granular soils show semi-elastic behavior at relatively low stress levels, and the deformation is associated with grain rearrangement, inter-grain slip, and rotation of particles [8, 32, 33]. Particle breakage usually occurs at high stress levels, and the disintegrated particles fill the inter-granular voids, leading to a further volume change [8, 9, 30]. To this end, an effective model is required to capture the coupling effect of initial density and particle crushing on the compression behavior of granular soils.

Three types of models have been proposed for estimating the compression behavior of granular soils: (1) models

✉ Xiusong Shi
qingsongsaint@gmail.com; xiusongshi@szu.edu.cn

Yiwen Zeng
zengyiwen2021@163.com

Jidong Zhao
jzhao@ust.hk

Xia Bian
xia.bian@hhu.edu.cn

Jiaying Liu
liujy@hzcu.edu.cn; liujiaying_222@outlook.com

[1] College of Civil and Transportation Engineering, Shenzhen University, Shenzhen, China

[2] Key Lab of Ministry of Education for Geomechanics and Embankment Engineering, Hohai University, Nanjing, China

[3] Department of Civil and Environmental Engineering, Hong Kong University of Science and Technology, Clearwater Bay, Kowloon, Hong Kong, China

[4] Department of Civil Engineering, Hangzhou City University, Hangzhou, China

based on the classic elastoplastic or hypoplastic framework [30, 34, 35]. For example, an incremental relationship between constrained modulus and effective stress is formulated by Pestana and Whittle [30] based on Limit Compression Curve (LCC). However, complicated numerical implementations are required for these types of models to be practically useful, which is inconvenient for engineers; (2) to reduce the computational complexity, phenomenological approaches based on laboratory observation are proposed by Pedroso et al. [36] and Sheng et al. [37]. For example, Sheng et al. [37] proposed a volume-stress model. This is done by incorporating a shifting stress into the LCC. It can well reproduce the non-linear compression behavior of granular soil with increasing stress levels. However, additional test data is required for soil with different initial densities to determine the shifting stress; (3) an empirical equation based on a postulate of active and inactive voids is established by Meidani et al. [38]. This model is effective for granular soils with different initial void ratios. Nevertheless, it is limited in capturing the deformation behavior at high stress level (e.g., 40 MPa for quartz sands).

In this study, an explicit compression model is proposed for granular soils. The effect of initial state on compressibility is captured by a novel equivalent void ratio, which incorporates a state variable to account for the evolving particle breakage and progressive yielding behavior. Verification reveals that the proposed model is effective in reproducing the compression behavior of various granular soils with a wide spectrum of initial densities and stress levels. No additional parameter is required for the simplified version of the model, which makes it suitable for practical applications.

2 Equivalent void ratio for the compressibility of granular soils

2.1 Equivalent concept

Thevanayagam and Mohan [39] introduced the equivalent concept to describe the contribution of fine (coarse) particles to the force chain of gap-graded granular soils with "coarse-in-fine" (or "fine-in-coarse") structure (e.g., sandy silts and silty sands). This is done by incorporating the equivalent void ratio into the model for pure coarse aggregates or fines (according to the relative dominance of fine and coarse particle). Key to the equivalent concept is to establish a state-dependent variable that can normalize the behavior of soils with different structures (e.g., fine content). It has been widely recognized that the equivalent void ratio proposed by Thevanayagam and Mohan [39] and their coworkers [40, 41] is effective in capturing the mechanical behavior of granular mixtures, such as critical state line [42, 43], small strain stiffness [44, 45], compressibility [46], liquefaction resistance [47–49] and permeability [50]. To the authors' knowledge, the application of equivalent void ratio concept is only limited to gap-graded soils, and its application to geo-materials with a continuous grading is seldom reported. Inspired by the traditional equivalent concept, a novel equivalent void ratio is proposed in the sequel to capture the compression behavior of various types of granular soils with different initial densities.

2.2 Equivalent void ratio for granular materials

Figure 1 presents a typical isotropic compression curve of granular soils (data from Lee and Seed [51]). Evidently, for a given stress level, the compressibility decreases with an increase of the initial density. Moreover, It indicates a good geometric similarity of the compression curves of sand with different initial void ratios. Note that, the analogous behavior of various granular materials is well reported by previous researchers based on both isotropic compression tests [8, 9, 37] and one-dimensional compression tests [13, 16]. Thus, for the sake of convenience, the compression curves of a given granular soil with various initial densities are collectively termed as Normal Compression Lines, NCLs herein regardless of bounding condition. Additionally, the definition of effective stress σ' in this study is corresponding to the loading condition. For example, σ' = confining stress for isotropic compression tests, and it denotes effective vertical stress when estimating the 1-D compression behavior. A schematic diagram for NCLs is shown in Fig. 1b, it is seen that they are approximately parallel at a very low stress level (10^{-2}-10^{-1} MPa). As the stress increases, NCLs with various initial densities gradually converge due to the progressive yielding that leads to a transition from semi-elastic to elasto-plastic behavior. They finally approach the LCC at a very high stress level (10^{1}-10^{2} MPa), indicating a negligible effect of initial density. This is interpreted by the evolution of particle breakage at high stress levels: the disintegrated finer grains provide a surrounding cushion pressure on the larger aggregates, and the relatively uniform contact network prevents them from further breakage, resulting in an ultimate Particle Size Distribution (PSD) and analogous compression behavior regardless of initial density [24, 30, 52–55].

Figures 1a and 1b shows a smooth variation on the curvature of NCLs across the whole range of initial density, indicating a continuous variation of soil fabric. In this case, one NCL with an arbitrary initial density (termed as the Reference Compression Line, RCL herein) may provide a good reference for estimating the state-dependent

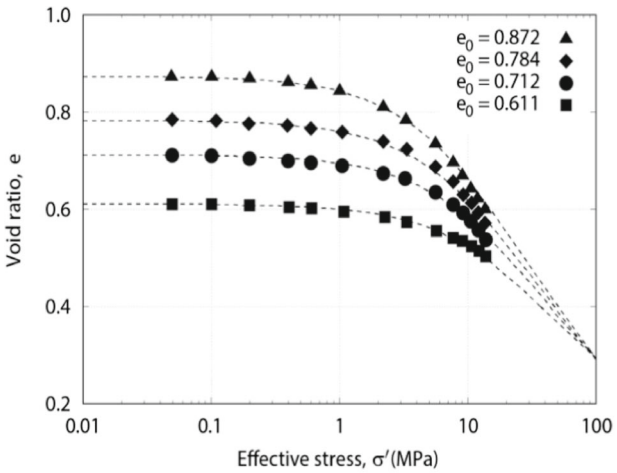

(a) Typical compression curves (data from [15])

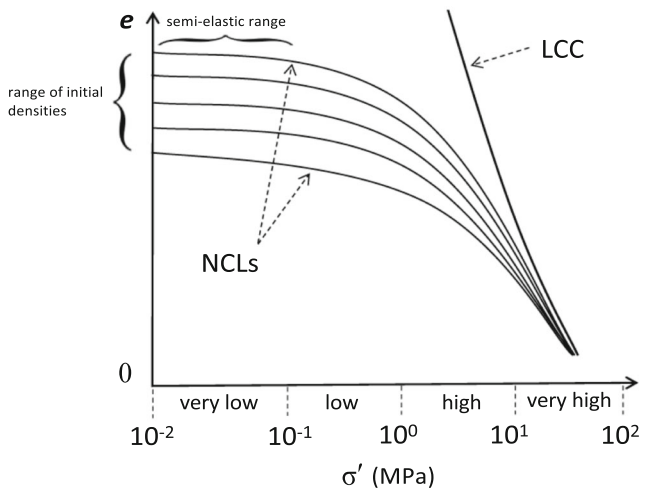

(b) Schematic diagram for the NCLs

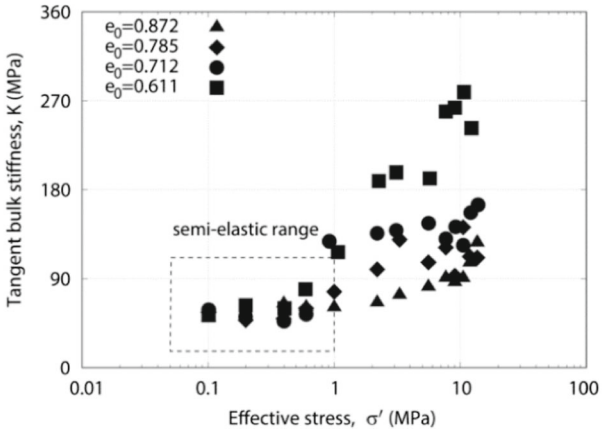

(c) Relationship between effective stress and tangent bulk stiffness (data from [15])

Fig. 1 Typical compression data of a granular soil with various initial densities and schematic diagram for the NCLs

compression behavior of the granular soil with various initial densities. Considering that the difference between the curvature of NCLs and that of the RCL is attributed to the initial packing arrangement and the evolution of yielding (refers to the irrecoverable fabric change of granular soil, which generates plastic volumetric deformation), a new equivalent void ratio is proposed in the sequel to capture this effect and normalize NCLs into the RCL.

The tangent bulk stiffness [$K = -\Delta\sigma'/\Delta\ln(1 + e)$] is further adopted to quantify the compressibility of granular soils. The relationship between σ' and K of Sacramento river sand (data from [51]) are presented in Fig. 1c. It is seen that the value of K is independent on initial void ratio within semi-elastic range (10^{-2} to 10^{-1} MPa), which indicates a negligible effect of initial density on the compressibility [4, 10, 56]. In this case, the NCL (defined as any compression line that is different from the RCL) can be reproduced by directly translating the RCL. Thus, the corresponding equivalent void ratio is formulated as

$$e^* = e + \Delta e_0 \tag{1}$$

where e^* represents the equivalent void ratio of granular soil, which is consistent to the current void ratio on RCL (red dashed line in Fig. 2) according to the mentioned equivalent concept. $e_{0,r}$ is the initial void ratio on RCL. e_0 and e are the initial and current void ratio of the predicted NCL (black dashed line in Fig. 2), respectively. $\Delta e_0 = e_{0,r} - e_0$ denotes the difference between RCL and NCL at the initial state of compression. As shown in Fig. 2, Eq. (1) refers to a negligible effect of initial density on the curvature of NCL (compared with the RCL) throughout the compression process. However, particle breakage may occur with an increasing stress level, which leads to a

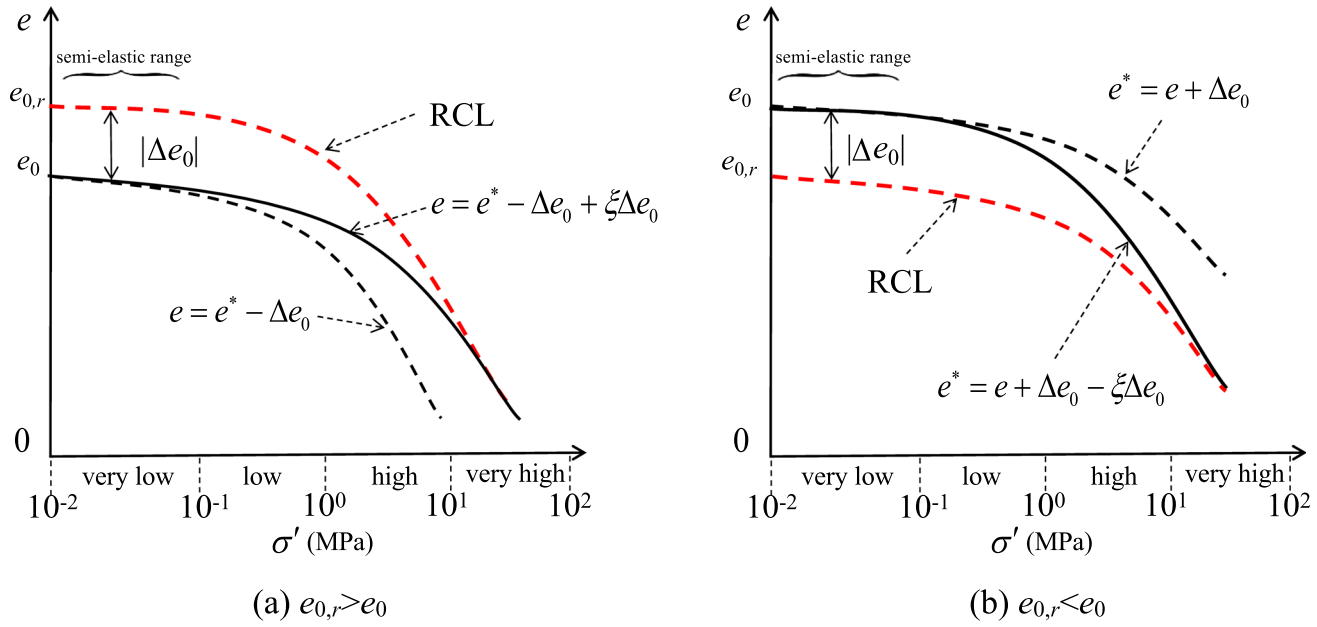

Fig. 2 Schematic diagram for the equivalent void ratio

convergence of the NCL and RCL. In this case, Eq. (1) is obviously not effective in describing the compressibility of granular soils. Therefore, a state variable ξ is introduced to capture the coupling effect of initial density and fabric change on the curvature of NCL, and the equivalent void ratio is revised as

$$e^* = e + \Delta e_0 - \xi \Delta e_0 \tag{2}$$

where $\xi\ \Delta e_0$ controls the evolving curvature of NCLs and is responsible for the coupling effect of initial state and progressive yielding. The evolution and detailed expression of ξ will be further addressed in the sequel.

3 Equivalent Compression Curve for granular materials

3.1 Reference Compression Line

Sheng et al. [37] reported that NCLs can be well captured by introducing different shifting stress (depends on the initial density) into the LCC. This method is straightforward and has been widely adopted for evaluating the deformation behavior of granular soils [57, 58]. For the sake of simplicity, the compression equation proposed by Sheng et al. [37] is adopted as the RCL to be used in conjunction with the proposed equivalent void ratio:

$$\ln e = \ln N - \lambda \ln\left(\frac{\sigma' + \sigma'_s}{\sigma'_r}\right) \tag{3}$$

where e and σ' are the current void ratio and effective stress, respectively. σ'_r = 1 MPa is a unit reference stress. λ and N denote the slope and intersection of the LCC, i.e., $\ln e = \ln N - \lambda \ln(\sigma'/\sigma'_r)$, respectively. σ'_s is a shifting stress related to curvature of the RCL:

$$\sigma'_s = \left(\frac{N}{e_{0,r}}\right)^{\frac{1}{\lambda}} - \sigma'_{0,r} \tag{4}$$

where $\sigma'_{0,r}$ is correlated with the initial compression data point of the RCL.

3.2 Equivalent compression curve

Considering that the difference between NCLs and the RCL is captured by proposed equivalent void ratio [Eq. (2)]. It is reasonable that NCLs could be normalized by directly substituting e^* into Eq. (3), which gives a new Equivalent Compression Curve (ECC) of granular soils:

$$\ln e^* = \ln N - \lambda \ln\left(\frac{\sigma' + \sigma'_s}{\sigma'_r}\right) \tag{5}$$

According to Eq. (2), the coupling effect of initial density and particle breakage is considered by introducing a state variable. Therefore, the ECC provides an explicit compression model for granular materials. Combining Eqs. (2) and (5) yields:

$$e = \exp\left(\ln N - \lambda \ln\left(\frac{\sigma' + \sigma'_s}{\sigma'_r}\right)\right) - \Delta e_0 + \xi \Delta e_0 \tag{6}$$

Note that other compression models for granular soil [30, 34, 36, 38] can also be adopted as optional RCL. Nevertheless, the value of ξ may be different if other reference model is utilized. The validation will be presented

to demonstrate that NCLs of various granular soils can be normalized by using the adopted RCL.

3.3 The expression of state variable ξ

Experimental results compiled from literature are utilized to further investigate the evolution of state variable ξ [51, 59–61]. Note that the value of ξ can be explicitly calculated according to Eqs. (2) and (5). Detailed soil properties and values of model parameters are given in Tables 1, 2, respectively.

The yielding of granular materials is directly correlated with the volumetric deformation (or current void ratio). Thus, the relationship between test results of state variable ξ and void ratio are shown in Fig. 3. It is seen that the ξ values of sand with different initial densities are close to zero at a low stress level, which is consistent with Eq. (1). Then, ξ increase continually as stress level rises (decrease of void ratio) and approach 1 regardless of initial density. A schematic diagram for the variation of e^* with current state and the corresponding nonlinear compression behavior is presented in Fig. 4. It is seen that $\xi = 0$ ($e^* = e + \Delta e$) when $e = e_0$ ($\sigma' = 0$), indicating a negligible effect of initial density on the compressibility. Notably, Eq. (2) is reduced to $e^* = e$ when $\xi = 1$, leading to an intersection between NCLs and RCL. The corresponding stress is termed as break down stress (σ'_b), which is related to the ultimate PSD of granular materials [4, 9, 56].

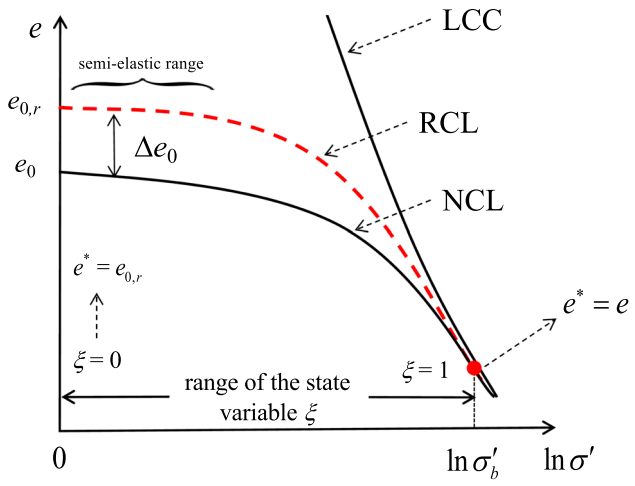

Fig. 4 Schematic diagram for the evolution of ξ and the corresponding compression behavior

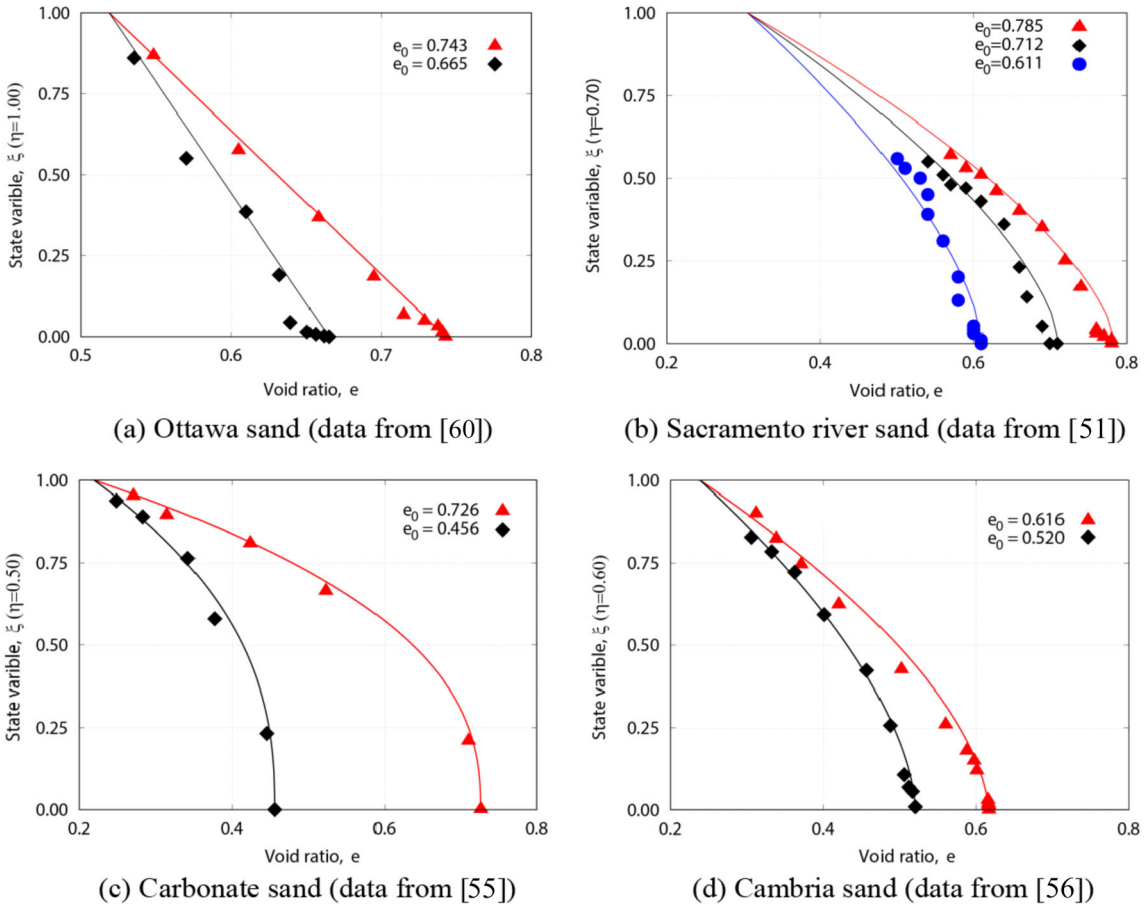

Fig. 3 Correlations between the state variable ξ and void ratio e

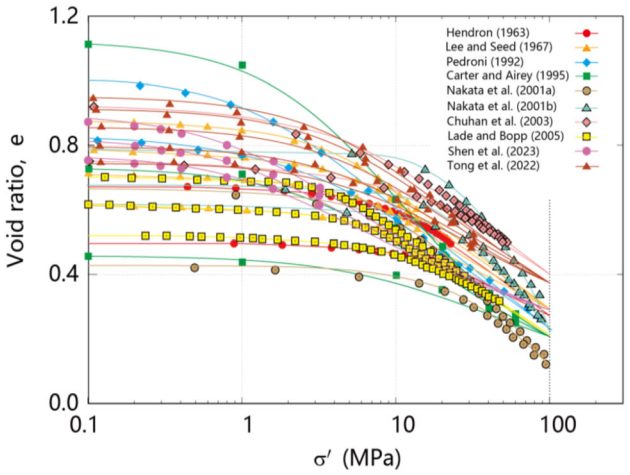

Fig. 5 Measured data (dots) and the trend lines of NCLs (lines)

Compression data of different granular soils are summarized in Fig. 5 to evaluate the value of σ_b' [10, 11, 13, 16, 30, 51, 59, 61–63]. The basic soil properties are given in Table 1. It is seen that the break down stress varies with the nature of soil particles (e.g., mineralogy, particle shape, roughness, and PSD). In detail, the value of σ_b' for fragile materials such as calcareous sand [13, 16] is generally lower than that of quartz sand [10, 11, 16]. Besides, the σ_b' might also be affected by the boundary condition and loading rate [19, 38]. However, NCLs all tend to intersect before 100 MPa regardless of the mentioned factors, which may provide an approximate reference for evaluating the evolving curvature of NCLs and the corresponding value of ξ. To this end,σ_b' 100 MPa is tentatively adopted, which will be further validated in the sequel. Note that the value of σ_b' for soil with high particle strength (e.g., rounded silica sand) might be higher than 100 MPa [9]. In this case, σ_b' = 1000 MPa is suggested for a more reliable prediction.

According to experimental results (Fig. 3), an inverse correlation is found between the value of ξ and the current void ratio. Moreover, ξ should meet the following requirements: (1) the curvature of NCLs is analogous to that of

Table 1 Basic physical properties of granular soils from literature

Soils		C_u	D_{50} (mm)	e_{min}	e_{max}	Mineralogy	Particle shape	Reference
Ottawa sand		1.50	0.14	0.63	0.83	Q	sR	De Souza [60]
Wabash river sand		3.00	0.56	0.43	0.69	Q	sA-sR	Hendron [63]
Sacramento river sand		1.50	0.22	0.61	1.03	F-Q	sA-sR	Lee and Seed [51]
Chattahoochee river sand		2.50	0.37	0.61	1.10	Q	sA	Vesic and Clough [55]
Toyoura sand		1.50	0.17	0.58	0.98	Q	sA	Miura N et al. [56]
Quiou sand		4.50	0.70	0.78	1.20	Ca	A	Pestana and Whittle [30], data cited from Pedroni (1992)
Carbonate sand		–	–	0.41	1.21	C	–	Carter and Airey [59]
Sillica sand		3.29	0.76	0.43	0.86	Q	A	Nakata et al. [10]
Toyoura sand		1.31	0.20	0.61	0.98	Q	R	Nakata et al. [11]
Mono-quartz sand		1.30	–	–	–	Q	R-sR	Chuhan et al. [62]
Cambria sand		–	–	0.50	0.79	Q	sA-R	Lade and Bopp [61]
Sillica sand	S1	1.58	3.20	–	–	Q	–	Zhang et al. [28]
	S2	1.14	1.01	–	–	Q	–	
	S3	3.60	1.49	–	–	Q	–	
Light-expanded clay aggregate		1.21	1.44	–	–	–	–	Guida G et al. [64]
Rockfill material	S1	1.00	2.50	–	–	–	sA-sR	Xiao et al. [17]
	S2	1.00	5.00	–	–	–	sA-sR	
Carbonate sand		1.38	1.12	1.82	1.13	Ca	A	Xiao et al. [65]
Carbonate silty sand		3.23	0.73	0.72	1.15	Ca	–	Tong et al. [16]
Calcareous gravelly sand		10.00	0.98	0.74	1.30	C	A	Shen et al. [13]

A=angular, R=round, sA=subangular, sR=subround,Q=siliceous (quartz), Ca=calcareous, C=carbonaceous, F=feldspar

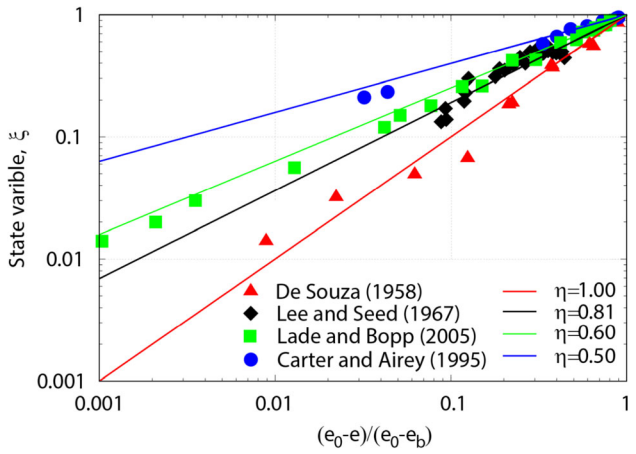

Fig. 6 Correlation between the state variable ξ with the best fitted value of η and $(e_0\text{-}e)/(e_0\text{-}e_b)$ of compression tests

RCL at a very low stress level ($e = e_0$), leading to a zero value of ξ; (2) the effect of initial density is negligible when the compression loading equals to the breakdown stress. In this case, the value of ξ should be 1. A simple power function is tentatively adopted to capture the evolution of ξ:

$$\xi = \left(\frac{e_0 - e}{e_0 - e_b}\right)^{\eta} \rightarrow \ln \xi = \eta \ln\left(\frac{e_0 - e}{e_0 - e_b}\right) \tag{7}$$

where e_b represents the void ratio at σ_b'. η is a parameter controlling the sensitivity of ξ to the void ratio. The simulated curves with best fitted η are presented in Fig. 3 and Fig. 6 (double logarithmic plot). It is seen that the evolution of ξ is well captured by the proposed equation, which reveals that η is a material constant that is independent of the initial state and stress level. Additionally, the experimental data of different crushable granular materials from Zhang et al. [28], Guida et al. [64], Xiao et al., [17] and

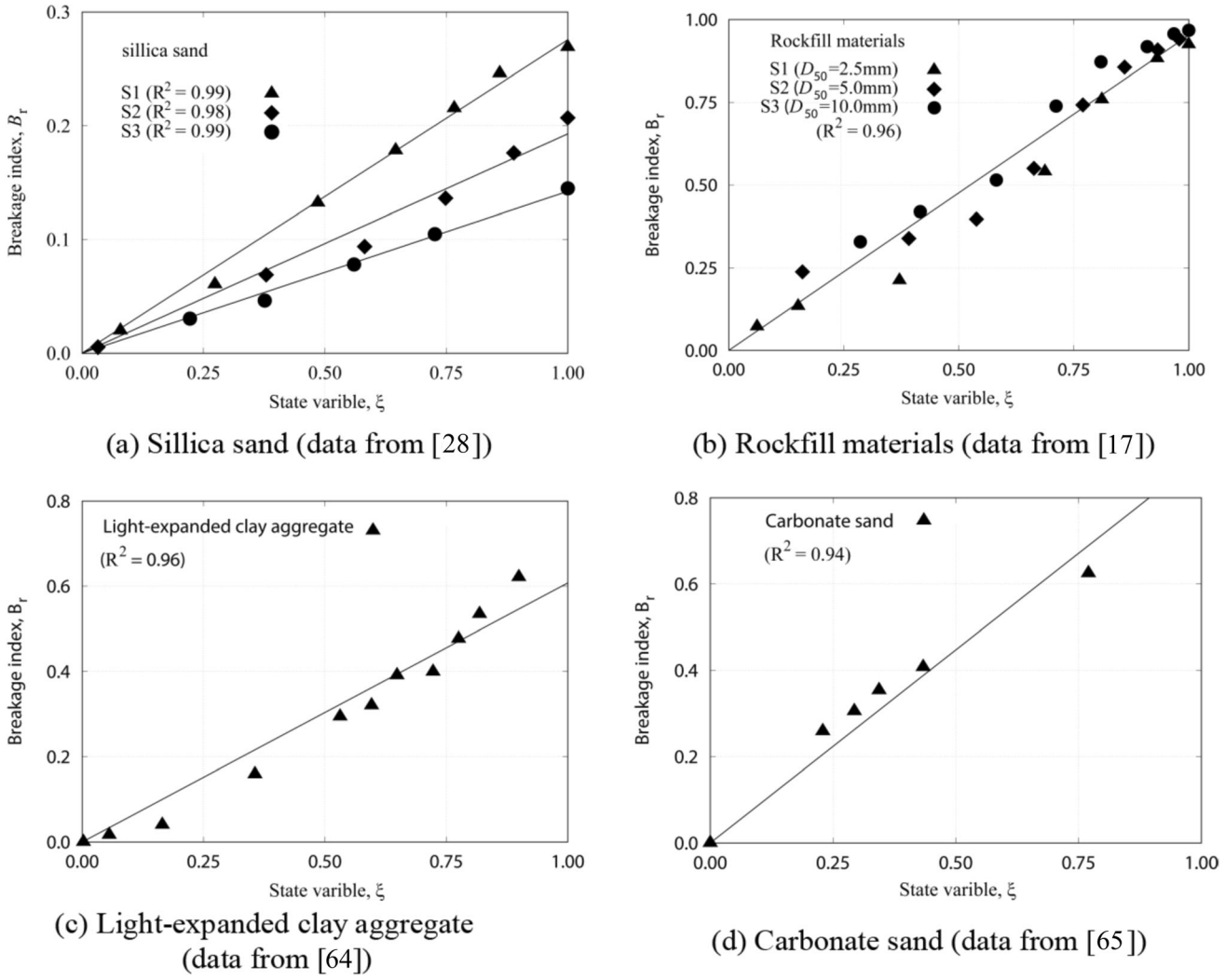

Fig. 7 Correlation between the state variable ξ and the breakage index B_r

Table 2 Values of model parameters for granular soils from literature

Soils	$e_{0,r}$	λ	N	σ'_s(MPa)	σ'_b(MPa)	η	Reference
Ottawa sand	0.800	0.29	2.12	28.6	100	1.00	De Souza [60]
Sacramento river sand	0.872	0.50	3.25	13.8	100	0.70	Lee and Seed [51]
Chattahoochee river sand	0.957	0.49	2.65	8.0	100	0.62	Vesic and Clough [55]
Toyoura sand	0.825	0.45	3.76	19.3	100	0.80	Miura N et al. [56]
Quiou sand	0.995	0.45	2.05	4.9	100	0.53	Pestana and Whittle [30], data cited from Pedroni (1992)
Carbonate sand	1.113	0.59	3.45	6.7	100	0.50	Carter and Airey [59]
Sillica sand	0.668	0.91	13.50	27.2	100	0.50	Nakata et al. [10]
Mono-quartz sand	0.880	0.39	2.67	17.1	100	0.68	Chuhan et al. [62]
Cambria sand	0.700	0.69	6.71	26.5	100	0.60	Lade and Bopp [61]
Carbonate silty sand	0.952	0.37	2.12	6.71	100	0.70	Tong et al. [16]
Calcareous gravelly sand	0.898	0.27	1.01	1.54	100	0.63	Shen et al. [13]

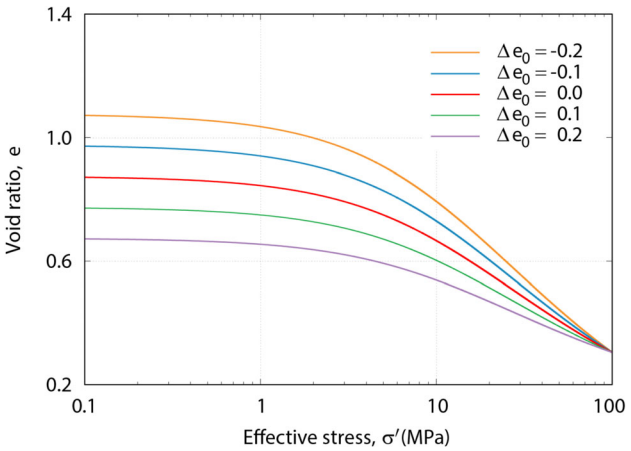

Fig. 8 Simulations of the compression curves with different values of Δe_0

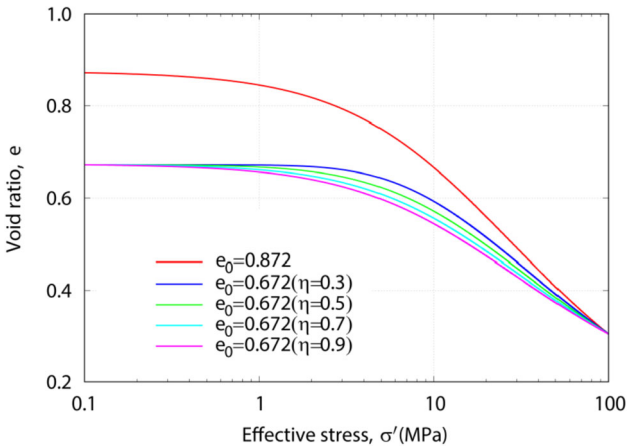

Fig. 9 Simulations of the compression curves with different values of η

Xiao et al., [65] (see Table 1 for detailed soil properties) are adopted to further explain the physical meaning of ξ. The values of ξ are calculated based on the Eq. (7) and $\eta = 1.0$ is adopted for the mentioned materials. The evolution of ξ against the relative breakage index B_r [66] (detailed descriptions are presented in Appendix) is given in Fig. 7. It shows a good linear relationship, which indicates that the effect of initial density on the curvature of NCLs is directly correlated with the evolution of particle breakage, and it can be effectively quantified by the proposed state variable.

Table 3 Values of model parameters for the parameter analysis

Series	$e_{0,r}$	λ	N	σ'_s(MPa)	σ'_b(MPa)	η	Δe_0
Series-1	0.872	0.50	3.25	13.8	100	1.0	0.20, 0.10, 0.00, -0.10, -0.20
Series-2						0.3, 0.5, 0.7, 0.9	0.20

4 Model parameters

4.1 Model parameters and their determination

Four material constants are required for the proposed model: λ, N,σ'_s and η. At least two conventional compression tests are required for the determination of those parameters. In detail, the compression data of a specimen with a given initial void ratio is utilized as the RCL. The corresponding compression parameters (λ and N) can be calibrated by best fitting the test data [30, 37], and the shifting stress, σ'_s is directly calculated according to

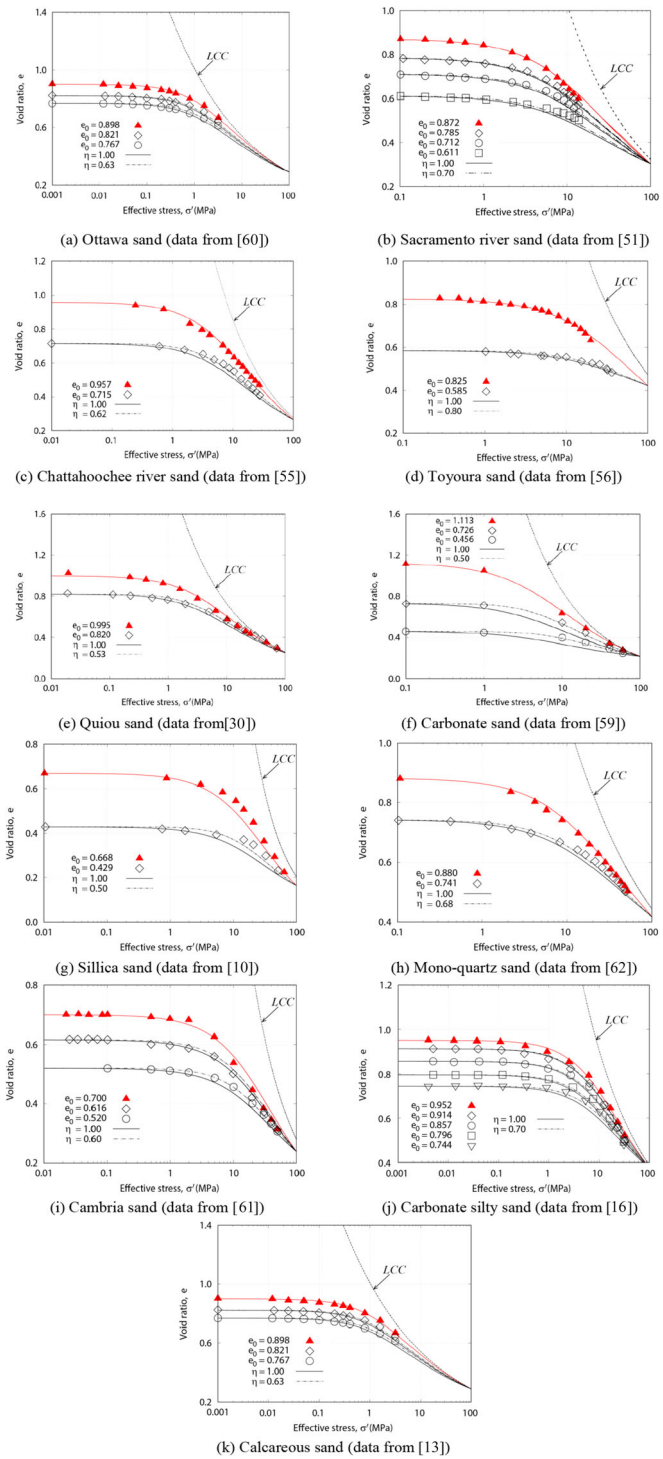

Fig. 10 Comparison of the model predictions and measured data from literature

Eq. (4). η is a structure parameter related to the evolution of particle breakage and corresponding progressive yielding behavior during compression, which depends on the average particle fragmentation strength (controlled by mineralogy and particle shape) and particle size distribution of granular material. As shown in Fig. 3, the value of η can be readily determined by the compression results of a specimen of with another initial density based on Eq. (7).

4.2 Parameter study of the proposed model

In this section, the effect of initial density and structure parameter is evaluated. The values of model parameters are

given in Table 2. The $e_{0,r}$ = 0.872 is assigned for the RCL, and the corresponding model parameters are consistent with that of Sacramento river sand from Lee and Seed [51]. The specimen is compressed from 0.1 MPa to the σ'_b (i.e., 100 MPa).

Figure 8 shows the effect of initial density (Series-1) on the simulated compression curves of granular soils. Five different values of Δe_0 (-0.2, -0.1, 0, 0.1, and 0.2) are considered. The results indicate that the compressibility of granular soils remains nearly constant at a low stress level ($\sigma' \leq 1$ MPa). However, as the stress increases, NCLs become concave downward and tend to converge at σ'_b regardless of the initial density.

The effect of structure parameter (Series-2) is simulated, and the results are presented in Fig. 9. The values of η are 0.3, 0.5, 0.7, and 0.9, respectively. Δe_0 = 0.2 is assigned for the compression model. The semi-elastic range is found gradually reduced (increase in crushability) with a rising η value, indicating that the structural parameter controls the evolution of particle breakage and the progressive yielding behavior with rising stress levels.

5 Simplified model and its validation

The compression test data of eleven different granular soils under isotropic [51, 55, 56, 59, 61] and one-dimensional [10, 13, 16, 30, 60, 62] compression loading are compiled from existing literature and utilized for the model validation. The basic soil properties are summarized in (Table 1).

5.1 Verification of the proposed model

The model parameters for the RCL are calibrated using data of soil samples with a high initial void ratio (Table 3). Note that σ'_b = 100 MPa is adopted for all eleven different granular soils. The comparisons between the predicted curves with the best fitted η (dashed line) and test results

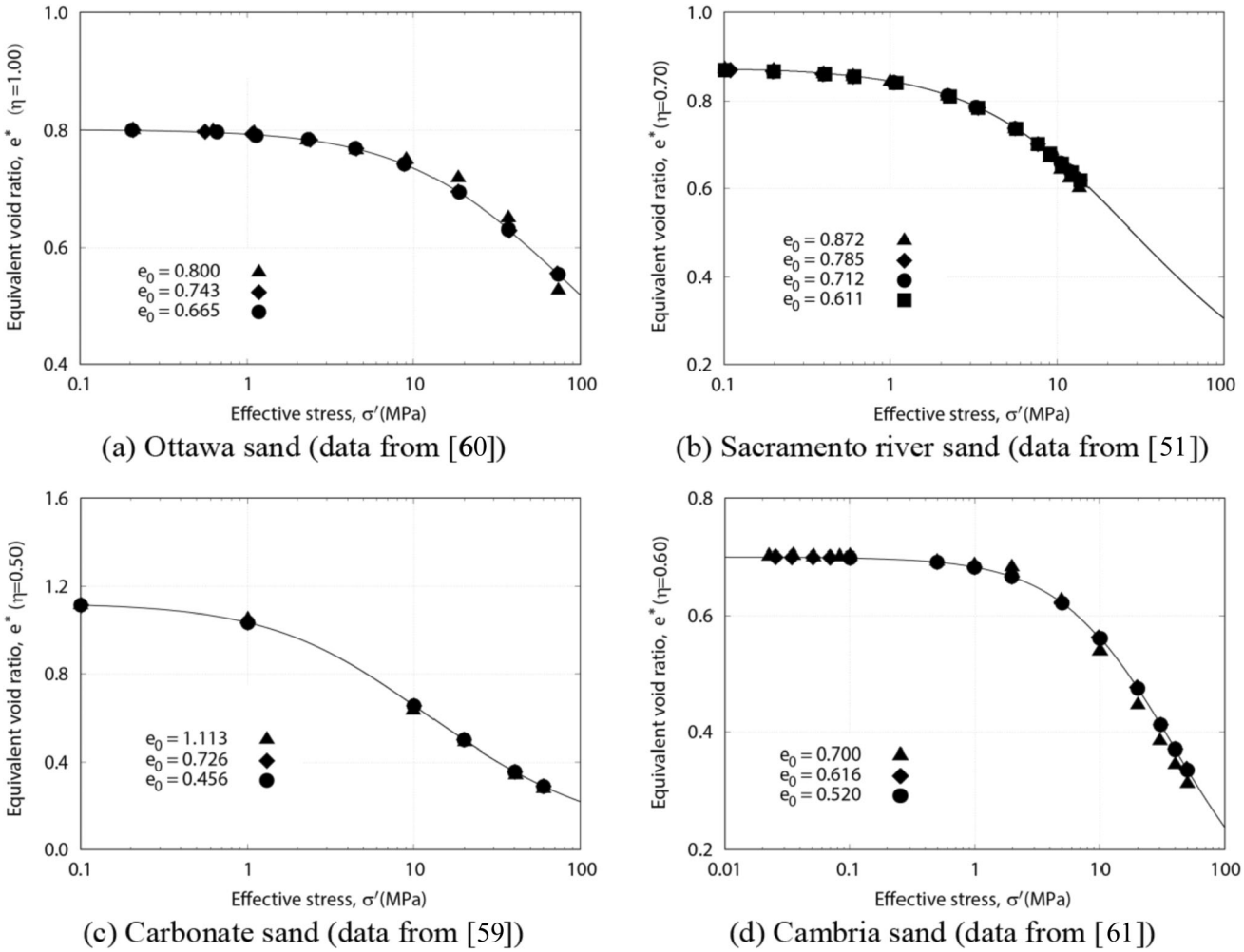

Fig. 11 Comparison of measured data and the equivalent compression curves

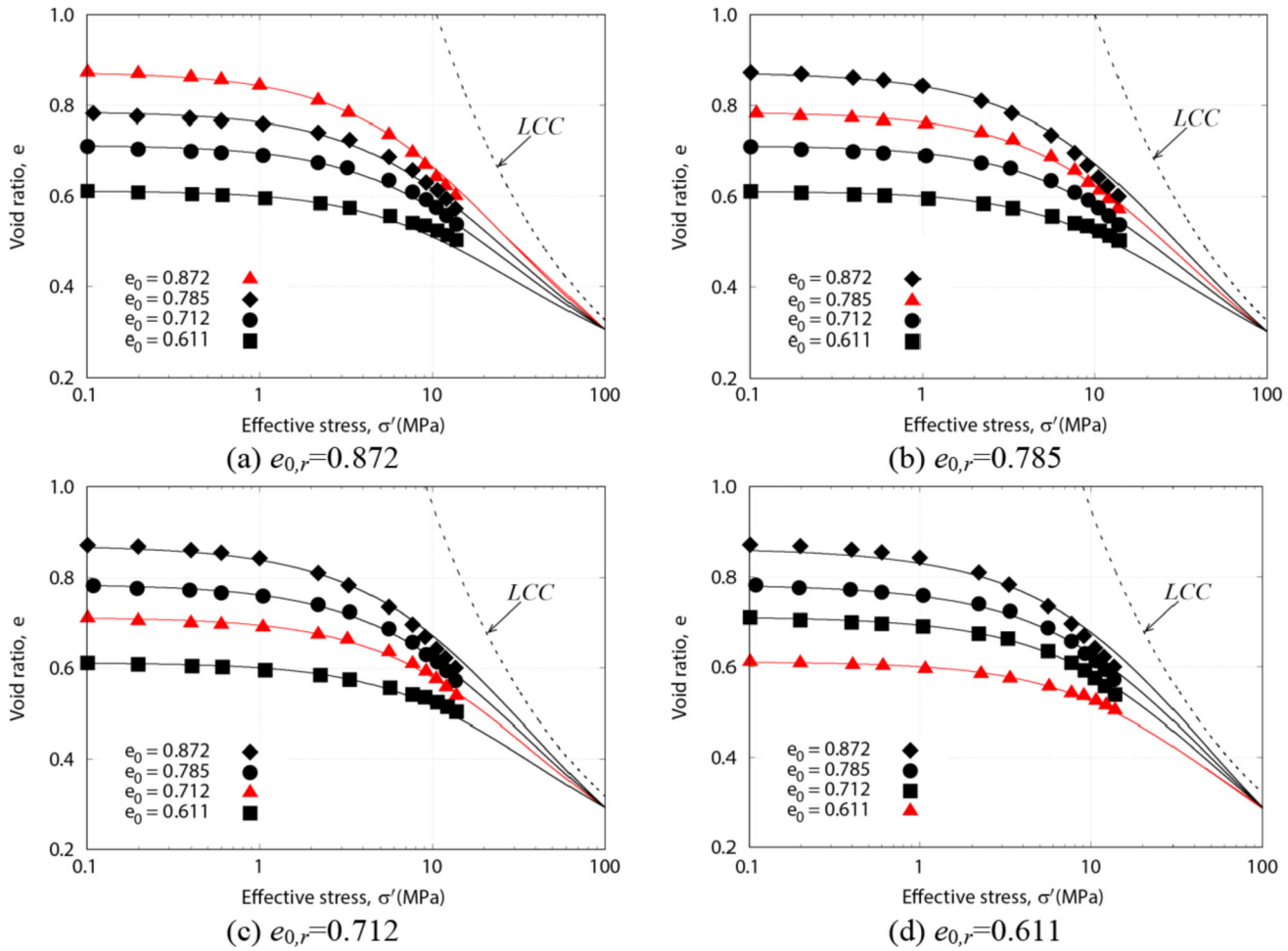

Fig. 12 Comparison of the model predictions and measured data on Sacramento river sand (data from [51]) with four different initial void ratio

Table 4 Values of model parameters (with different RCLs)

Soil	$e_{0,r}$	λ	N	σ'_s(MPa)	σ'_b(MPa)	η	Reference
Sacramento river sand	0.872	0.50	3.25	13.8	100	0.70	Lee and Seed [51]
	0.785	0.49	3.10	16.4			
	0.712	0.48	2.90	18.6			
	0.611	0.47	2.80	25.5			

(dots) are shown in Fig. 10. Note that the solid red dots and lines are associated with the RCL. It can be seen that the simulated results are consistent with compression data under both isotropic [51, 55, 56, 59, 61] and anisotropic [10, 13, 16, 30, 60, 62] loading condition, indicating a satisfactory capacity of the proposed model in capturing the non-linear compression behavior of different types of granular soils with a broad spectrum of densities and stress levels.

The calculated curves and experimental results of four different types of granular soils are shown in Fig. 11 in terms of the equivalent void ratio versus effective stress. It is seen that the compression curves of granular soils with various initial densities can be well normalized by the proposed ECC.

Moreover, the experimental data [51] and curves predicted using different RCLs (red lines) are presented in Fig. 12. The values of model parameter for the RCLs are summarized in Table 4. Note that the value of η is independent on the $e_{0,r}$. It shows that the compression behavior can be well captured by using the RCLs with different

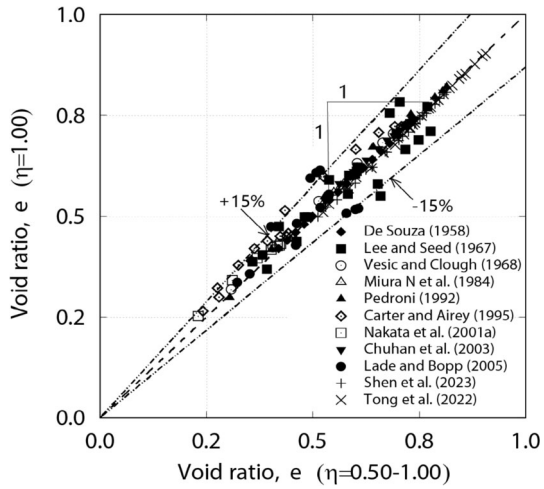

Fig. 13 Comparison between model calculations with the best fitted η and $\eta = 1.0$

initial densities, which further verifies the introduced equivalent concept.

5.2 Simplification of the proposed model

As can be seen from Table 3, the structure parameter η of different types of granular materials varies in a narrow range (0.5-1.0). Besides, the simulated results in Fig. 9 show that there is only a slight difference among the curves calculated with various values of η. In this case, η = 1.0 can be adopted for simplicity, which leads to a linear relationship between the state variable and current void ratio:

$$\xi = \frac{e_0 - e}{e_0 - e_b} \tag{8}$$

According to Eq. (8), no additional parameter is required for the proposed ECC (compared with the reference model). Figure 13 shows the comparison between model calculations with the best fitted η and η = 1.0. It indicates that the deviation between those simulated results is within a narrow range (± 15%). The model predictions (η = 1.0, solid lines) are also presented in Fig. 10. It confirms a satisfactory performance of the simplified ECC. This suggests that the proposed model works reasonably and robustly well for a wide spectrum of granular soils with various particle shapes, mineralogy, and PSD. It should be noted that the simplified model might ignore the effect of basic soil properties on the evolution of grain crushing during compression process. However, it can greatly reduce the complexity of the proposed model and yet provide an adequate simulation, which can well satisfy the engineering requirements.

6 Conclusions

In this study, a new equivalent void ratio is introduced for granular soils and its capability has been evaluated by the experimental data compiled from the existing literature. Conclusions of this work are summarized as follows:

1) A novel equivalent void ratio is proposed to capture the coupling effect of initial state and particle breakage on compressibility of granular soils.
2) An explicit Equivalent Compression Curve is formulated by directly incorporating the equivalent void ratio into a reference model, and the compression curves of granular soils with different initial densities can be well normalized by the ECC.
3) Validation shows that no additional parameter (compared with the reference model) is required for the simplified version of the compression model. The three model parameters can be readily determined from one conventional compression test.

Appendix

The relative breakage index B_r is expressed as

$$B_r = B_t / B_p \tag{14}$$

where B_p is breakage potential, which is defined as the area between the initial PSD of granular materials with a lower bound by No. 200 sieve (0.074 mm). B_t denotes the area between the initial and final PSD curve.

Acknowledgements This study was partially supported by the National Natural Science Foundation of China (under Grant no. 52278346; Grant no. 12272334).

Author Contribution Z.Y.W. wrote the original draft of the manuscript. S.X.S. contributed to the conception, design and writing-review of this research. Z.J.D., B.X. and L.J.Y. contributed to the writing-review and editing of this research. All authors reviewed the previous versions of the manuscript. The final manuscript was approved by all authors.

Data availability statement All data generated and analyzed during this work are included in this published article. No datasets were generated or analysed during the current study.

Declarations

Conflict of Interest The authors declare no competing interests.

References

1. He SH, Goudarzy M, Ding Z, Sun Y (2023) Strength, deformation, and particle breakage behavior of calcareous sand: role of anisotropic consolidation. J Geotech Geoenviron Eng

149(3):04023002. https://doi.org/10.1061/JGGEFK.GTENG-10501
2. Irani N, Lashkari A, Tafili M, Wichtmann T (2022) A state-dependent hyperelastic-plastic constitutive model considering shear-induced particle breakage in granular soils. Acta Geotech 17(11):5275–5298. https://doi.org/10.1007/s11440-022-01636-z
3. Li Y, Cui Y, Hu X, Lu Z, Guo J, Wang Y, Zhou X (2024) Glacier retreat in Eastern Himalaya drives catastrophic glacier hazard chain. Geophys Res Lett. https://doi.org/10.1029/2024GL108202
4. Nimbalkar S, Indraratna B, Dash SK, Christie D (2012) Improved performance of railway ballast under impact loads using shock mats. J Geotech Geoenviron Eng 138(3):281–294. https://doi.org/10.1061/(ASCE)GT.1943-5606.0000598
5. Wang P, Yin ZY, Wang ZY (2022) Micromechanical investigation of particle-size effect of granular materials in biaxial test with the role of particle breakage. J Eng Mech 148(1):04021133. https://doi.org/10.1061/(ASCE)EM.1943-7889.0002039
6. Xiao Y, Liu H, Ding X, Chen Y, Jiang J, Zhang W (2016) Influence of particle breakage on critical state line of rockfill material. Int J Geomech 16(1):04015031. https://doi.org/10.1061/(ASCE)GM.1943-5622.0000538
7. Levin F (2021) Time-dependent compression behavior of sands under oedometric conditions. J Geotech Geoenviron Eng 147(12):04021144. https://doi.org/10.1061/(ASCE)GT.1943-5606.0002664
8. Mesri G, Vardhanabhuti B (2009) Compression of granular materials. Can Geotech J 46(4):369–392. https://doi.org/10.1139/T08-123
9. Mun W, McCartney JS (2017) Roles of particle breakage and drainage in the isotropic compression of sand to high pressures. J Geotech Geoenviron Eng 143(10):04017071. https://doi.org/10.1061/(ASCE)GT.1943-5606.0001770
10. Nakata Y, Hyodo M, Hyde AF, Kato Y, Murata H (2001) Microscopic particle crushing of sand subjected to high pressure one-dimensional compression. Soils Found 41(1):69–82. https://doi.org/10.3208/sandf.41.69
11. Nakata Y, Kato Y, Hyodo M, Hyde AF, Murata H (2001) One-dimensional compression behaviour of uniformly graded sand related to single particle crushing strength. Soils Found 41(2):39–51. https://doi.org/10.3208/sandf.41.2_39
12. Seo D, Sohn C, Cil MB, Buscarnera G (2021) Evolution of particle morphology and mode of fracture during the oedometric compression of sand. Géotechnique 71(10):853–865. https://doi.org/10.1680/jgeot.18.P.300
13. Shen J, Chen X, Wang X, Wang X, Qin Y, Wu H (2023) Compression responses and particle breakage of calcareous granular material in reclaimed islands. Powder Technol 418:118277. https://doi.org/10.1016/j.powtec.2023.118277
14. Shi XS, Liu K, Yin J (2021) Effect of initial density, particle shape, and confining stress on the critical state behavior of weathered gap-graded granular soils. J Geotech Geoenviron Eng 147(2):04020160. https://doi.org/10.1061/(ASCE)GT.1943-5606.000244
15. Singh S, Zurakowski Z, Dai S, Zhang Y (2021) Effect of grain crushing on the hydraulic conductivity of tailings sand. J Geotech Geoenviron Eng 147(12):04021143. https://doi.org/10.1061/(ASCE)GT.1943-5606.0002667
16. Tong CX, Dong ZL, Sun Q, Zhang S, Zheng JX, Sheng D (2022) On compression behavior and particle breakage of carbonate silty sands. Eng Geol 297:106492. https://doi.org/10.1016/j.enggeo.2021.106492
17. Xiao Y, Meng M, Daouadji A, Chen Q, Wu Z, Jiang X (2020) Effects of particle size on crushing and deformation behaviors of rockfill materials. Geosci Front 11(2):375–388. https://doi.org/10.1016/j.gsf.2018.10.010
18. Yu-ran X, Yongfu X, Ao-xun W (2022) One-dimensional compression characteristics of uniformly graded sand under high stresses. Granular Matter 24(2):60. https://doi.org/10.1007/s10035-022-01213-x
19. Zeng K, Liu H (2023) Experimental study on the time-dependent oedometric compression behavior of calcareous sand. J Geotech Geoenviron Eng 149(5):04023025. https://doi.org/10.1061/JGGEFK.GTENG-10739
20. Ciantia MO, Arroyo M, Calvetti F, Gens A (2015) An approach to enhance efficiency of DEM modelling of soils with crushable grains. Géotechnique 65(2):91–110. https://doi.org/10.1680/geot.13.P.218
21. Cil MB, Sohn C, Buscarnera G (2020) DEM modeling of grain size effect in brittle granular soils. J Eng Mech 146(3):04019138. https://doi.org/10.1061/(ASCE)EM.1943-7889.0001713
22. Fu R, Hu X, Zhou B (2017) Discrete element modeling of crushable sands considering realistic particle shape effect. Comput Geotech 91:179–191. https://doi.org/10.1016/j.compgeo.2017.07.016
23. Hall SA, Bornert M, Desrues J, Pannier Y, Lenoir N, Viggiani G, Bésuelle P (2010) Discrete and continuum analysis of localised deformation in sand using X-ray μCT and volumetric digital image correlation. Géotechnique 60(5):315–322. https://doi.org/10.1680/geot.2010.60.5.315
24. McDowell GR, de Bono JP (2013) On the micro mechanics of one-dimensional normal compression. Géotechnique 63(11):895–908. https://doi.org/10.1680/geot.12.P.041
25. Shi K, Zhu F, Zhao J (2024) The critical state of crushable granular sand. Acta Geotech 19(1):1–18. https://doi.org/10.1007/s11440-023-02112-y
26. Shi XS, Nie J, Zhao J, Gao Y (2020) A homogenization equation for the small strain stiffness of gap-graded granular materials. Comput Geotech 121:103440. https://doi.org/10.1016/j.compgeo.2020.103440
27. Xiong H, Zhang Z, Bao X, Wu H, Yin ZY, Chen X (2024) Micromechanical analysis of particle shape effect on suffusion of gap-graded soils. Comput Geotech 165:105925. https://doi.org/10.1016/j.compgeo.2023.105925
28. Zhang JR, Hu Y, Zhang BW, Liu YZ (2015) Fractal behavior of particle-size distribution during particle crushing of quartz sand and gravel. Chin J Geotech Eng. 37(5):784–791
29. Zhang T, Zhang C, Yang Q, Fu R (2020) Inter-particle friction and particle sphericity effects on isotropic compression behavior in real-shaped sand assemblies. Comput Geotech 126:103741. https://doi.org/10.1016/j.compgeo.2020.103741
30. Pestana JM, Whittle AJ (1995) Compression model for cohesionless soils. Géotechnique. 45(4):611–631
31. Shi XS, Zhao J, Gao Y (2021) A homogenization-based state-dependent model for gap-graded granular materials with fine-dominated structure. Int J Numer Anal Methods Geomech 45(8):1007–1028. https://doi.org/10.1002/nag.3189
32. Wang H, Cui YJ, Zhang F, Liu J (2022) Effect of grain breakage on the compressibility of soils. Acta Geotech 17(3):769–778. https://doi.org/10.1007/s11440-021-01256-z
33. Xiao Y, Liu H, Chen Q, Ma Q, Xiang Y, Zheng Y (2017) Particle breakage and deformation of carbonate sands with wide range of densities during compression loading process. Acta Geotech 12(5):1177–1184. https://doi.org/10.1007/s11440-017-0580-y
34. Bauer E (1996) Calibration of a comprehensive hypoplastic model for granular materials. Soils Found 36(1):13–26. https://doi.org/10.3208/sandf.36.13
35. Tengattini A, Das A, Einav I (2016) A constitutive modelling framework predicting critical state in sand undergoing crushing and dilation. Géotechnique 66(9):695–710. https://doi.org/10.1680/jgeot.14.P.164

36. Pedroso DM, Sheng D, Zhao J (2009) The concept of reference curves for constitutive modelling in soil mechanics. Comput Geotech 36(1–2):149–165. https://doi.org/10.1016/j.compgeo.2008.01.009
37. Sheng D, Yao Y, Carter JP (2008) A volume-stress model for sands under isotropic and critical stress states. Can Geotech J 45(11):1639–1645. https://doi.org/10.1139/T08-085
38. Meidani M, Chang CS, Deng Y (2017) On active and inactive voids and a compression model for granular soils. Eng Geol 222:156–167. https://doi.org/10.1016/j.enggeo.2017.03.006
39. Thevanayagam S, Mohan S (2000) Intergranular state variables and stress-strain behaviour of silty sands. Géotechnique 50(1):1–23. https://doi.org/10.1680/geot.2000.50.1.1
40. Thevanayagam S (2000) Liquefaction potential and undrained fragility of silty soils. In proceedings of the 12th world conference earthquake engineering. New Zealand Society of Earthquake Engineering. Wellington. New Zealand.
41. Thevanayagam S, Liang J (2001) Shear wave velocity relations for silty and gravely soils. Proc, 4th Int Conf on Soil Dynamics and Earthquake Engineering. Univ of Missouri Rolla, San Diego, pp 1–15
42. Sun Z, Chu J, Xiao Y (2021) Formulation and implementation of an elastoplastic constitutive model for sand-fines mixtures. Int J Numer Anal Methods Geomech 45(18):2682–2708. https://doi.org/10.1002/nag.3282
43. Thevanayagam S, Shenthan T, Mohan S, Liang J (2002) Undrained fragility of clean sands, silty sands, and sandy silts. J Geotech Geoenviron Eng 128(10):849–859. https://doi.org/10.1061/(ASCE)1090-0241(2002)128:10(849)
44. Goudarzy M, König D, Schanz T (2016) Small strain stiffness of granular materials containing fines. Soils Found 56(5):756–764. https://doi.org/10.1016/j.sandf.2016.08.002
45. Rahman MM, Cubrinovski M, Lo SR (2012) Initial shear modulus of sandy soils and equivalent granular void ratio. Geomech Geoengin 7(3):219–226. https://doi.org/10.1080/17486025.2011.616935
46. Shi XS, Zhao J (2020) Practical estimation of compression behavior of clayey/silty sands using equivalent void-ratio concept. J Geotech Geoenviron Eng 146(6):04020046. https://doi.org/10.1061/(ASCE)GT.1943-5606.0002267
47. Lashkari A (2014) Recommendations for extension and re-calibration of an existing sand constitutive model taking into account varying non-plastic fines content. Soil Dyn Earthquake Eng 61:212–238. https://doi.org/10.1016/j.soildyn.2014.02.012
48. Lashkari A (2016) Prediction of flow liquefaction instability of clean and silty sands. Acta geotech 11(5):987–1014. https://doi.org/10.1007/s11440-015-0413-9
49. Lashkari A, Shourijeh PT, Khorasani SSS, Irani N, Rahman MM (2022) Effects of over-consolidation history on flow instability of clean and silty sands. Acta geotech 17(11):4989–5007. https://doi.org/10.1007/s11440-022-01502-y
50. Shi XS, Zeng Y, Shi C, Ma Z, Chen W (2022) Evaluation of hydraulic conductivity of gap-graded granular soils based on equivalent void ratio concept. Acta Geotech 17(9):3839–3854. https://doi.org/10.1007/s11440-022-01484-x
51. Lee KL, Seed HB (1967) Drained strength characteristics of sands. J Soil Mech Found Div 93(6):117–141. https://doi.org/10.1061/JSFEAQ.0001048
52. Liu J, Zhou W, Ma G, Yang S, Chang X (2020) Strong contacts, connectivity and fabric anisotropy in granular materials: a 3D perspective. Powder Technol 366:747–760. https://doi.org/10.1016/j.powtec.2020.03.018
53. Ma G, Chen Y, Yao F, Zhou W, Wang Q (2019) Evolution of particle size and shape towards a steady state: Insights from FDEM simulations of crushable granular materials. Comput Geotech 112:147–158. https://doi.org/10.1016/j.compgeo.2019.04.022
54. Owolabi AT, Torres-Cruz LA, Vermeulen N (2021) Effect of gradation and particle shape on the limiting compression curves of sand-sized siliceous materials. J Geotech Geoenviron Eng 147(7):06021007. https://doi.org/10.1061/(ASCE)GT.1943-5606.0002574
55. Vesić AS, Clough GW (1968) Behavior of granular materials under high stresses. J Soil Mech Found Div ASCE 94(3):661–688. https://doi.org/10.1061/JSFEAQ.0001134
56. Miura N, Murata H, Yasufuku N (1984) Stress-strain characteristics of sand in a particle-crushing region. Soils Found 24(1):77–89. https://doi.org/10.3208/sandf1972.24.77
57. Liu L, Yao Y, Luo T, Zhou A (2020) A constitutive model for granular materials subjected to a large stress range. Comput Geotech 120:103408. https://doi.org/10.1016/j.compgeo.2019.103408
58. Yao YP, Liu L, Luo T, Tian Y, Zhang JM (2019) Unified hardening (UH) model for clays and sands. Comput Geotech 110:326–343. https://doi.org/10.1016/j.compgeo.2019.02.024
59. Carter JP, Airey DW (1995) The engineering behaviour of cemented marine carbonate soils. Int J Rock Mech Min 32(3):A108A
60. De Souza J M (1958) Compressibility of sand at high pressure. MS thesis, MIT, 63-64.
61. Lade PV, Bopp PA (2005) Relative density effects on drained sand behavior at high pressures. Soils Found 45(1):1–13. https://doi.org/10.3208/sandf.45.1_1
62. Chuhan FA, Kjeldstad A, Bjørlykke K, Høeg K (2003) Experimental compression of loose sands: relevance to porosity reduction during burial in sedimentary basins. Can Geotech J 40(5):995–1011. https://doi.org/10.1139/t03-050
63. Hendron AJ (1963) The Behavior of Sand in One-Dimensional Compression, PhD thesis, niv of Illinois 50–89
64. Guida G, Casini F, Viggiani GM, Ando E, Viggiani G (2018) Breakage mechanisms of highly porous particles in 1D compression revealed by X-ray tomography. Géotechniq Lett 8(2):155–160. https://doi.org/10.1680/jgele.18.00035
65. Xiao Y, Yuan Z, Chu J et al (2019) Particle breakage and energy dissipation of carbonate sands under quasi-static and dynamic compression. Acta Geotech 14:1741–1755. https://doi.org/10.1007/s11440-019-00790-1
66. Hardin BO (1985) Crushing of soil particles. J Geotech Eng 111(10):1177–1192. https://doi.org/10.1061/(ASCE)0733-9410(1985)111:10(1177)
67. Wu Y, Yamamoto H, Cui J, Cheng H (2020) Influence of load mode on particle crushing characteristics of silica sand at high stresses. Int J Geomech 20(3):04019194. https://doi.org/10.1061/(ASCE)GM.1943-5622.0001600
68. Zhang C, Zhao Y, Bai Q (2022) 3D DEM method for compaction and breakage characteristics simulation of broken rock mass in goaf. Acta geotech 17(7):2765–2781. https://doi.org/10.1007/s11440-021-01379-3